Quantum Chemical Investigation of Mechanisms of Silane Oxidation

Mary M. Mader*,† and Per-Ola Norrby*,‡

Contribution from the Department of Chemistry, Grinnell College, Grinnell, Iowa 50112, and Department of Medicinal Chemistry, The Royal Danish School of Pharmacy, Universitetsparken 2, DK-2100 Copenhagen, Denmark

Received April 21, 2000. Revised Manuscript Received December 13, 2000

Abstract: Several mechanisms for the peroxide oxidation of organosilanes to alcohols are compared by quantum chemical calculations, including solvation with the PCM method. Without doubt, the reaction proceeds via anionic, pentacoordinate silicate species, but a profound difference is found between in vacuo and solvated reaction profiles, as expected. In the solvents investigated (CH_2Cl_2 and MeOH), the most favorable mechanism is addition of peroxide anion to a fluorosilane (starting material or formed in situ), followed by a concerted migration and dissociation of hydroxide anion. In the gas phase, and possibly in very nonpolar solvents, concerted addition−migration of H_2O_2 to a pentacoordinate fluorosilicate is also plausible.

Introduction

The oxidation chemistry of silanes has been exploited in natural products syntheses, as silicon's ability to act as a "masked" hydroxyl group allows it to be used in situations in which the presence of an alcohol is unfavorable.[1] For example, in reactions of Fleming[1] and Chan, the α-carbon is employed as a nucleophile, a difficult feat even with a protected alcohol. The oxidation requires that at least one of the silicon substituents is an electronegative heteroatom. Thus, the Tamao oxidation employs an alkoxysilane[2] (eq 1), whereas the Fleming protocol[3] converts a phenylsilane to a fluoro- or carboxysilane before the actual oxidation (eq 2). The oxidizing agents most frequently

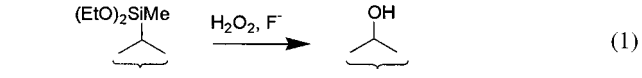

(1)

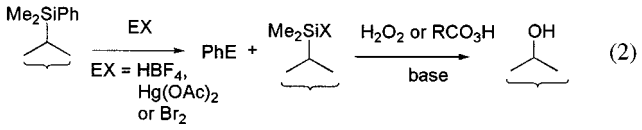

(2)

used are hydrogen peroxide, *m*-chloroperbenzoic acid, or peracetic acid. Additional fluoride (KF and/or KHF_2) is required in many, but not all, existing protocols. Basic conditions (KH, *tert*-butylhydroperoxide, and TBAF) have been employed as well, allowing a wide range of alkyl and aryl substituents on silicon.[4] More recently, silicon substituted with a 2-pyridyl group has been oxidized under Tamao conditions (H_2O_2, KF), and fluoride was demonstrated to play a critical role in this reaction.[5] The substitution pattern and reaction conditions show substantial variation, but the following elements are common to all protocols: (a) The silicon is substituted with an electronegative heteroatom, presumably to activate it to nucleophilic addition. (b) Additional fluoride ion is often required. The role of the fluoride has been debated,[6,7] and may vary with different substitution patterns, but the strong bond between silicon and fluorine should play an important role in stabilizing hypervalent states (intermediates or transition states). (c) The oxidizing agent is always a peroxide. The thermodynamic driving force for the reaction results from breaking the weak O−O bond while simultaneously forming strong Si−O and C−O bonds. In analogy with accepted hydroboration−oxidation mechanisms,[8] the rate-determining step is presumed to be the breaking of the O−O bond with simultaneous migration of an alkyl substituent from silicon to oxygen.

Both Fleming and Tamao have proposed mechanisms for the oxidation. Tamao et al. have shown that stable fluorosilanes of the type $PhSiMe_{3-n}F_n$ are not oxidized by H_2O_2 unless additional fluoride is present in the reaction mixture.[6,7] In addition, the formation of pentacoordinate fluorosilicates was observed by following the change of the methyl proton chemical shifts by ^1H NMR. In Tamao's proposed mechanism, an initially formed pentavalent fluorosilane is attacked by hydrogen peroxide to form a hexacoordinate transition state, which undergoes concerted migration of an alkyl group from silicon to oxygen (Scheme 1, path C). No signals corresponding to a hexavalent

† Grinnell College.; Current Address: Eli Lilly and Company, Lilly Corporate Center, Drop Code 1523, Indianapolis, IN 46285. E-mail: mader_mary@lilly.com.

‡ Royal Danish School of Pharmacy. Current address: Technical University of Denmark, Department of Organic Chemistry, Building 201, Kemitorvet, DK-2800 Lyngby, Denmark. E-mail: okpon@pop.dtu.dk.

(1) For applications in the synthesis of natural products, see: (a) Ahmar, M.; Duyck, C.; Fleming, I. *Pure Appl. Chem.* **1994**, *66*, 2049−2052. (b) Magar, S. S.; Fuchs, P. L. *Tetrahedron Lett.* **1991**, *32*, 5713−5716. (c) Barrett, A. G. M.; Head, J.; Smith, M. L.; Stock, N. S.; White, A. J. P.; Williams, D. J. *J. Org. Chem.* **1999**, *64*, 6005−6018. (d) Peng, Z.-H.; Woerpel, K. A. *Org. Lett.* **2000**, *2*, 1379−1381. (e) Mader, M. M.; Edel, J. C. *J. Org. Chem.* **1998**, *63*, 2761−2764.

(2) Tamao, K.; Ishida, N.; Tanaka, T.; Kumada, M. *Organometallics* **1983**, *2*, 1694−1696.

(3) Fleming, I.; Henning, R.; Parker, D. C.; Plaut, H. E.; Sanderson, P. E. J. *J. Chem. Soc., Perkin Trans. 1* **1995**, 317−336.

(4) Smitrovich, J. H.; Woerpel, K. A. *J. Org. Chem.* **1996**, *61*, 6044−6046.

(5) Itami, K.; Mitsudo, K.; Yoshida, J-i. *J. Org. Chem.* **1999**, *64*, 8709−8714.

(6) For reviews, see: (a) Tamao, K.; Hayashi, T.; Ito, Y. In *Frontiers of Organosilicon Chemistry*; Bassindale, A. R., Gaspar, P. P., Eds.; The Royal Society of Chemistry: Cambridge, 1991; pp 197−207. (b) Tamao, K. *Advances in Silicon Chemistry*; JAI Press: Greenwich, CT, 1996; Vol. 3, pp 1−62.

(7) Tamao, K.; Kakui, T.; Akita, M.; Iwahara, T.; Kanatani, R.; Yoshida, J.; Kumada, M. *Tetrahedron* **1983**, *39*, 983−990.

(8) Brown, H. C. *Organic Synthesis via Boranes*; John Wiley and Sons: New York, 1975.

10.1021/ja001400p CCC: $20.00
Published on Web 02/10/2001

Scheme 1

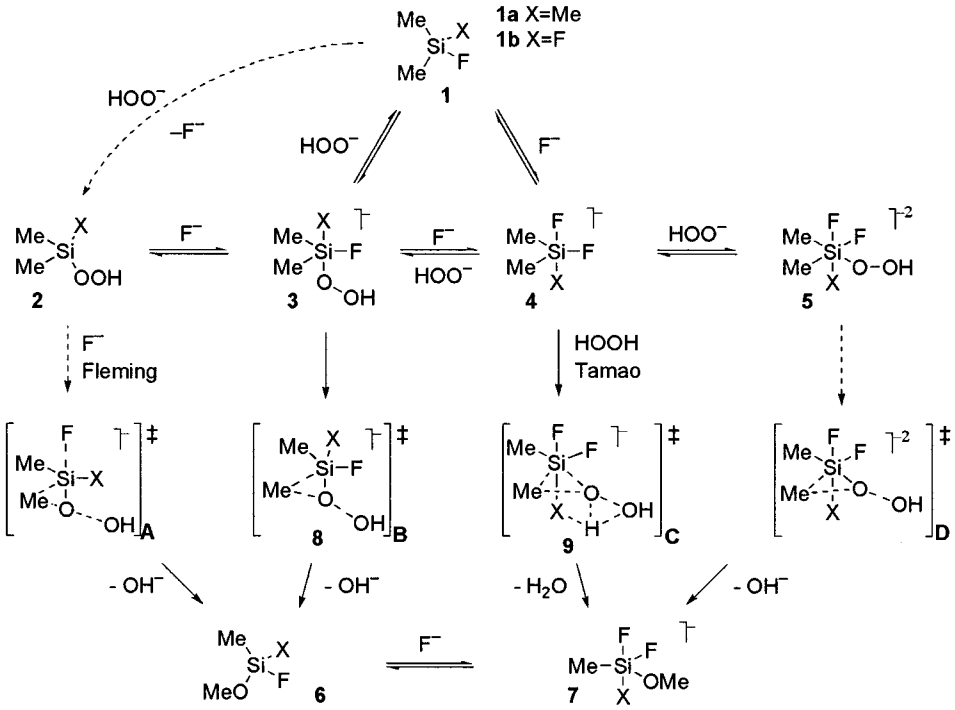

intermediate were observed. However, silicon is known to form stable hexacoordinated complexes when the substituents are sufficiently electronegative.[9] A path involving a hexacoordinate peroxo silicate as a transient intermediate is also compatible with the reported observations, and has therefore been considered in the current study (Scheme 1, path D).

Fleming's mechanism,[10] like Tamao's, recognizes the importance of the electron-withdrawing group on silicon, but suggests that the acetate, alkoxide, or fluoride serves as a leaving group upon attack by peroxide or peracid. The peroxysilane is then attacked by fluoride anion, inducing a concerted alkyl migration from silicon to oxygen (Scheme 1, path A). Although Fleming has worked extensively to optimize the oxidation chemistry under a variety of conditions, he has not reported detailed mechanistic studies. The mechanisms of Tamao and Fleming conflict both in the coordination number of the silicon and in the mode of attack, but they both rationalize the need for fluoride ion, and share the common feature that the rate-limiting step is a concerted addition−migration. An alternative mechanism can be formulated: formation of a pentavalent fluoroperoxo silicate, with subsequent migration of an alkyl group (Scheme 1, path B). As this species can be directly formed from addition of peroxide anion to fluorosilane, this path may not require fluoride, but could be aided by fluoride under Curtin−Hammett conditions. Corriu has demonstrated that pentavalent silane species are more reactive than the tetravalent ones in nucleophilic displacements.[9,11] Thus, addition of fluoride to the initial silane followed by formation of the pentavalent peroxy silane through nucleophilic displacement would be compatible with known results. Alternatively, the pentavalent peroxide could be subject to rapid and reversible fluoride dissociation. Three groups have suggested similar mechanisms for related silane reactions. Damrauer's studies of rearrangements of chloromethyl trialkylsilanes (R_3SiCH_2Cl) showed dependence on fluoride ion, consistent with formation of a pentavalent intermediate.[12] Sakurai has effected conversion of trifluorosilanes to alcohols with trimethylamine-*N*-oxide, and proposed that the reaction occurs via a pentacoordinate silane by attack of oxygen on silicon followed by migration of an alkyl group from silicon. In this case, an excess of fluoride was not required.[13] Yoshida et al., in their development of the Tamao-type oxidation of 2-pyridyldimethylsilane, invoke a pentavalent silicon species to rationalize the experimentally determined dependence of the reaction on fluoride.[5] All of these proposals parallel the well-accepted mechanism for hydroboration rearrangements, in which the Lewis acidic boron becomes tetravalent upon attack by peroxide.[14]

Reactions at silicon have been investigated at ab initio and semiempirical levels.[9,15] Hypervalent silicon species have been confirmed computationally for a variety of processes, including silyl-mediated aldol reactions[16] and a variety of reactions involving attack by nucleophiles.[11,17,18] To clarify the mechanism of the oxidation of silanes to alcohols, we have performed

(9) For an extensive review of penta- and hexacoordinate silicon compounds, see: Chuit, C.; Corriu, R. J. P.; Reye, C.; Young, J. C. *Chem. Rev.* **1993**, *93*, 1371−1448.

(10) For a review that includes a discussion of possible mechanisms, see: Fleming, I. *Chemtracts: Org. Chem.* **1996**, 1−64.

(11) (a) Corriu, R. *Pure Appl. Chem.* **1988**, *60*, 99−106. (b) Corriu, R. In *Frontiers of Organosilicon Chemistry*; Bassindale, A. R., Gaspar, P. P., Eds.; The Royal Society of Chemistry: Cambridge, 1991; pp 185−196.

(12) Damrauer, R.; Danahey, S. E.; Yost, V. E. *J. Am. Chem. Soc.* **1984**, *106*, 7633−7634.

(13) Sato, K.; Kira, M.; Sakurai, H. *Tetrahedron Lett.* **1989**, *30*, 4375−4378.

(14) For ab initio studies of related borane systems, see: (a) Midland, M. M. *J. Org. Chem.* **1998**, *63*, 914−915. (b) Wang, X.; Li, Y.; Wu, Y.-D.; Paddon-Row: M. N.; Rondan, N. G.; Houk, K. N. *J. Org. Chem.* **1990**, *55*, 2601−2609.

(15) For reviews see: (a) Damrauer, R.; Hankin, J. A. *Chem. Rev.* **1995**, *95*, 1137−1160. (b) Holmes, R. R. *Chem. Rev.* **1990**, *90*, 17−31.

(16) (a) Gung, B. W.; Zhu, Z.; Fouch, R. A. *J. Org. Chem.* **1995**, *60*, 2860−2864. (b) Denmark, S. E.; Griedel, B. D.; Coe, D. M.; Schnute, M. E. *J. Am Chem. Soc.* **1994**, *116*, 7026−7043. (c) Sakurai, H. *Synlett* **1989**, *1*, 1.

(17) (a) Schlegel, H. B.; Skancke, P. N. *J. Am. Chem. Soc.* **1993**, *115*, 10916−10924. (b) Morgon, N. H.; Argenton, A. B.; da Silva, M. L. P.; Riveros, J. M. *J. Am. Chem. Soc.* **1997**, *119*, 1708−1716. (c) Brinkman, E. A.; Berger, S.; Brauman, J. I. *J. Am. Chem. Soc.* **1994**, *116*, 8304−8310. (d) Hensen, K.; Stumpf, T.; Bolte, M.; Näther, C.; Fleischer, H. *J. Am Chem. Soc.* **1998**, *120*, 10402−10408.

quantum chemical investigations of four postulated pathways for two different model systems. Some workers, including Yoshida, note that in alcohol, siloxane species $ROSiR'_3$ can be isolated in the absence of peroxide, and that this intermediate can undergo the rearrangement upon subsequent treatment with peroxide. For this work, we investigated mechanisms involving fluorosilanes in the presence of H_2O_2 or HOO^-; paths involving alkoxysilanes are the focus of ongoing computational efforts. In addition to intermediates, we have also located transition states for the postulated rate-limiting steps (O−O bond breaking and alkyl migration). The computed mechanisms with both basic and neutral hydroperoxide are consistent with Tamao's kinetic studies, confirming the order of reactivity for the fluorosilanes of the type $PhSiMe_{3-n}F_n$ to be $n = 2 \gg n = 1$, the need for additional fluoride in many cases, and the formation of pentavalent species.

Confirmation of the mechanism is potentially useful for further organosilane methodology development, and could possibly throw light on related reactions. In particular, verification of hypervalent silicates as intermediates is of special interest. Pentavalent siloxanes are synthetically useful and are the important reactive species in recently reported Hiyama−Tamao cross-coupling reactions,[19] and a pentavalent fluorosilicate has been developed as a fluoride source.[20] Synthetic methods more related to the currently investigated reaction could include development of silicon as a "masked" amine, as a synthetic analogue of the silane oxidation.

Methods

As our basic model system, we chose the reaction of trimethylfluorosilane (**1a**) with fluoride and hydrogen peroxide (possibly deprotonated), corresponding to the second step in the Fleming protocol. We also wanted to rationalize the rate acceleration obtained by employing two electronegative substituents. To this end, we also calculated the reaction path starting from dimethyldifluorosilane (**1b**). Difluorosilanes have been explicitly investigated by Tamao, and may be intermediates in reactions of dialkoxysilanes in the presence of excess fluoride. Conformational searches were conducted at low levels of theory, with a coarse selection at MNDO-d and refinement at HF/3-21G*, in Spartan 4.1 and 5.0.[21] Geometries were optimized at HF/6-31G*[22] using Gaussian94.[23] Initial transition state (TS) geometries were located by the linear synchronous transit, coordinate driving, or direct construction of a plausible geometry, followed by full refinement (at HF/6-31G*), in Gaussian94, Gaussian98,[24] or Jaguar.[25] Thermodynamic contributions were calculated from normal-mode analysis at HF/6-31G*, using a temperature of 298 K. Transition states and minima were verified to have exactly one and zero negative eigenvalues, respectively; all transition states displayed one imaginary frequency, 800−900 cm^{-1}. The lowest real frequency was larger than 50 cm^{-1} for all ground states. The effect of correlation[26] and diffuse[27] functions was estimated by single-point calculations at MP2/6-31G**, MP2/6-311+G**, and HF/6-31+G*. Solvation effects in two typical solvents, MeOH and CH_2Cl_2, were estimated at the gas-phase HF/6-31G* geometries by using the continuum solvation method PCM/DIR together with the HF/6-31+G* wave function.[28] The effect of a correlated treatment on final geometries was investigated by reoptimization of the HF/6-31G* structures at the B3LYP/6-31+G*[29] level. To determine if significant geometry changes would occur, selected structures were optimized in solvent as well, using the updated CPCM/UAHF method in Gaussian98.[24] A high-level correction, ΔHL, was calculated as the difference between a correlated calculation with a large, diffuse basis set and the HF/6-31+G* level (eq 3). Final free energies in solvent were then

$$\Delta\mathrm{HL} = E(\mathrm{MP2/6\text{-}311+G^{**}}) - E(\mathrm{HF/6\text{-}31+G^{*}}) \qquad (3)$$

obtained by combination of the PCM results (at gas-phase geometries or optimized in solvent) with the high-level correction and vibrational contribution (eq 4). It was necessary to calculate the latter contributions

$$G_{\mathrm{comp}} = \Delta\mathrm{HL} + \Delta G_{\mathrm{therm}}(\mathrm{HF/6\text{-}31G^{*}},\ 298\ \mathrm{K}) + G_{\mathrm{sol}}(\mathrm{PCM}) \qquad (4)$$

at the gas-phase geometries, as Gaussian does not allow determination of analytical frequencies with PCM. However, the gas-phase and solution structures are similar, so the change is believed to be minor.

Results

All HF/6-31G* structures, and energies calculated at various levels, are available as Supporting Information. In Table 1 can be found all relative energies, compared to starting materials of equivalent stoichiometries. For example, the energy of **3** is reported relative to that of separated **1** + HOO^-, whereas TS_C-**(9)** is compared to that of **1** + F^- + H_2O_2. The resulting reaction energies and activation barriers at various levels, including free energies calculated according to eq 4, can be found in Table 2.

The gas-phase potential energy profiles at different levels of theory for the two model systems are depicted in Figures 1 and 2. Comparing the other levels to the results from the correlated calculation with a diffuse basis set, two expected effects are immediately clear. First, barriers are strongly overestimated at the HF level. Second, failure to include diffuse functions led to severe basis set superposition errors (BSSE). These could in principle be alleviated by a counterpoise correction, but the

(18) (a) Damrauer, R.; Burggraf, L. W.; Davis, L. P.; Gordon, M. S. *J. Am. Chem. Soc.* **1988**, *110*, 6601−6606. (b) Davis, L. P.; Burggraf, L. W.; Gordon, M. S. *J. Am. Chem. Soc.* **1988**, *110*, 3056−3062. (c) Schmidt, M. W.; Windus, T. L.; Gordon, M. S. *J. Am. Chem. Soc.* **1995**, *117*, 7480−7486.

(19) (a) Brescia, M. R.; DeShong, P. *J. Org. Chem.* **1998**, *63*, 3156−3157. (b) Mowery, M. E.; DeShong, P. *J. Org. Chem.* **1999**, *64*, 1684−1688.

(20) Pilcher, A. S.; Ammon, H. L.; DeShong, P. *J. Am. Chem. Soc.* **1995**, *117*, 5166−5167.

(21) Spartan SGI version 5.0.3, Wavefunction Inc., 18401 von Karman, Suite 370, Irvine, CA 92715.

(22) (a) Hehre, W. J.; Ditchfield, R.; Pople, J. A. *J. Chem. Phys.* **1972**, *56*, 2257−2261. (b) Hariharan, P. C.; Pople, J. A. *Theor. Chim. Acta* **1973**, *28*, 213−222. (c) Gordon, M. S. *Chem. Phys.* **1980**, *76*, 163.

(23) Gaussian94 (Rev. B.2), Frisch, M. J.; Trucks, G. W.; Schlegel, H. B.; Gill, P. M. W.; Johnson, B. G.; Robb, M. A.; Cheeseman, J. R.; Keith, T. A.; Petersson, G. A.; Montgomery, J. A.; Raghavachari, K.; Al-Laham, M. A.; Zakrzewski, V. G.; Ortiz, J. V.; Foresman, J. B.; Cioslowski, J.; Stefanov, B. B.; Nanayakkara, A.; Challacombe, M.; Peng, C. Y.; Ayala, P. Y.; Chen, W.; Wong, M. W.; Andres, J. L.; Replogle, E. S.; Gomperts, R.; Martin, R. L.; Fox, D. J.; Binkley, J. S.; Defrees, D. J.; Baker, J.; Stewart, J. P.; Head-Gordon, M.; Gonzalez, C.; Pople, J. A. Gaussian, Inc.: Pittsburgh, PA, 1995.

(24) Gaussian98 (Rev. A.7), Frisch, M. J.; Trucks, G. W.; Schlegel, H. B.; Scuseria, G. E.; Robb, M. A.; Cheeseman, J. R.; Zakrzewski, V. G.; Montgomery, J. A., Jr.; Stratmann, R. E.; Burant, J. C.; Dapprich, S.; Millam, J. M.; Daniels, A. D.; Kudin, K. N.; Strain, M. C.; Farkas, O.; Tomasi, J.; Barone, V.; Cossi, M.; Cammi, R.; Mennucci, B.; Pomelli, C.; Adamo, C.; Clifford, S.; Ochterski, J.; Petersson, G. A.; Ayala, P. Y.; Cui, Q.; Morokuma, K.; Malick, D. K.; Rabuck, A. D.; Raghavachari, K.; Foresman, J. B.; Cioslowski, J.; Ortiz, J. V.; Baboul, A. G.; Stefanov, B. B.; Liu, G.; Liashenko, A.; Piskorz, P.; Komaromi, I.; Gomperts, R.; Martin, R. L.; Fox, D. J.; Keith, T.; Al-Laham, M. A.; Peng, C. Y.; Nanayakkara, A.; Gonzalez, C.; Challacombe, M.; Gill, P. M. W.; Johnson, B.; Chen, W.; Wong, M. W.; Andres, J. L.; Gonzalez, C.; Head-Gordon, M.; Replogle, E. S.; Pople, J. A. Gaussian, Inc.: Pittsburgh, PA, 1998.

(25) Jaguar 4.0; Schrodinger, Inc.: Portland, OR, 2000.

(26) Pople, J. A.; Binkley, J. S.; Seeger, R. *Int. J. Quantum. Chem.* **1976**, *S10*, 1.

(27) Frisch, M. J.; Pople, J. A.; Binkley, J. S. *J. Chem. Phys.* **1984**, *80*, 3265−3269.

(28) PCM/DIR version 2.0, courtesy of Dr. Maurizio Cossi and Professor Vincenzo Barone: Cossi, M.; Barone, V.; Cammi, R.; Tomasi, J. *Chem. Phys. Lett.* **1996**, *255*, 327−335. Note that this version of PCM differs substantially from the older PCM implemented in Gaussian94, and slightly from the more recent version in Gaussian98.

(29) (a) Becke, A. D. *J. Chem. Phys.* **1993**, *98*, 5648−5652. (b) Lee, C.; Yang, W.; Parr, R. G. *Phys. Rev. B* **1988**, *37*, 785−789. (c) Kohn, W.; Becke, A. D.; Parr, R. G. *J. Phys. Chem.* **1996**, *100*, 12974.

Table 1. Calculated Energies and Energy Components Relative to Starting Materials (**1** + reagents, fluoride and/or peroxide), in kJ/mol

	HF/6-31G* geometry								Opt[a] B3LYP/ 6-31+G*	Opt[a] G_{sol} CH_2Cl_2
	HF/ 6-31G*	HF/ 6-31+G*	ΔZPE	ΔG^b	G_{sol} MeOH	G_{sol} CH_2Cl_2	MP2/ 6-31G**	MP2/ 6-311+G**		
2a	126	31	4	19	−93	−78	120	−1	19	−61
3a	−164	−113	12	59	45	4	−229	−158	−153	16
4a	−289	−166	3	30	89	45	−334	−175	−169	36
5a	−31	135	11	93	181	143	−142	68	108	—[c]
6a	−245	−296	3	11	−395	−377	−243	−307	−265	—[c]
7a	−547	−459	7	50	−301	−328	−599	−485	−431	—[c]
8a	55	80	2	49	50	41	−124	−75	−63	68
9a	−1	127	5	82	264	203	−271	−99	−59	196
2b	122	29	6	21	−92	−77	116	−1	17	−59
3b	−228	−183	13	62	−27	−66	−285	−222	−197	−54
4b	−332	−204	4	33	53	6	−373	−208	−201	−2
5b	−101	171	14	97	198	174	−202	4	42	—[c]
6b	−248	−299	4	12	−393	−375	−243	−308	−265	—[c]
7b	−575	−496	6	50	−356	−381	−637	−528	−460	—[c]
8b	30	55	3	49	−20	−29	−153	−113	−95	19
9b	−48	84	8	89	178	127	−323	−147	−105	151

[a] Geometries optimized at this level. [b] Includes ΔZPE. [c] Not determined.

Table 2. Calculated Activation Barriers and Reaction Energies (kJ/mol)

reaction	MP2/ 6-31G**	MP2/ 6-311+G**	B3LYP[a]/ 6-31+G*	ΔG (eq 4) gas	MeOH	CH_2Cl_2	CH_2Cl_2[a]
1a + HOO^- ⇔ **2a** + F^-	120	−1	19	45	−93	−78	−61
2a + F^- ⇔ **3a**	−349	−158	−172	−163	138	83	77
3a + F^- ⇔ **4a** + HOO^-	−104	−17	−16	−62	44	41	19
4a + HOO^- ⇔ **5a**	192	243	276	298	91	98	—[b]
3a → **8a**	106	83	90	68	5	37	52
4a + H_2O_2 → **9a**	63	77	109	120	175	158	161
6a + F^- ⇔ **7a**	−356	−178	−166	−178	95	49	—[b]
1b + HOO^- ⇔ **2b** + F^-	116	−1	17	44	−92	−77	−59
2b + F^- ⇔ **3b**	−401	−221	−214	−222	65	12	5
3b + F^- ⇔ **4b** + HOO^-	−88	14	−4	−33	80	72	52
4b + HOO^- ⇔ **5b**	170	326	243	379	145	168	—[b]
3b → **8b**	132	109	102	100	7	37	73
4b + H_2O_2 → **9b**	50	61	95	109	125	120	153
6b + F^- ⇔ **7b**	−394	−220	−195	−225	37	−6	—[b]

[a] Geometries optimized at this level. [b] Not determined.

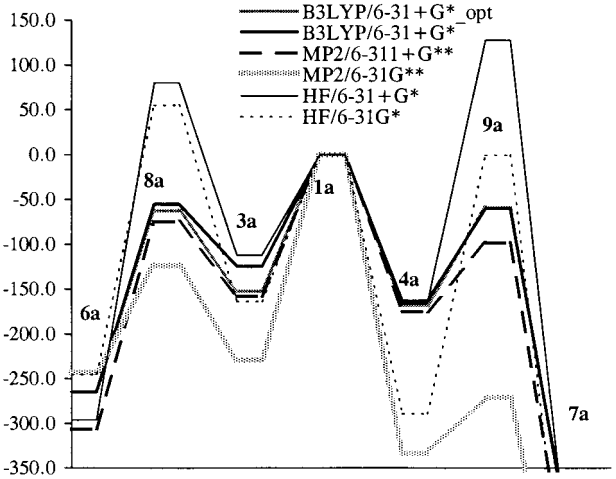

Figure 1. Potential energy profiles for oxidation of trimethyl fluorosilane (**1a**), kJ/mol.

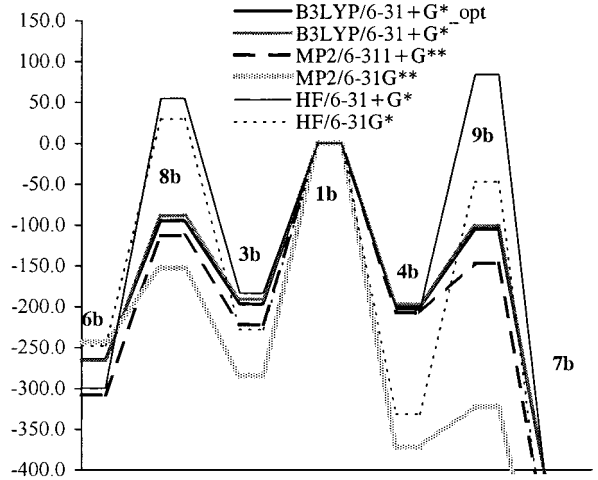

Figure 2. Potential energy profiles for oxidation of dimethyl difluorosilane (**1b**), kJ/mol.

procedures available to us also include the occupied orbitals of the partner and may thus overcompensate the stabilization. Instead, we have chosen to minimize the effects by saturating the basis set at the correlated level (MP2/6-311+G**). Gratifyingly, very similar results could be obtained at the B3LYP/6-31+G* level. Optimization at this level only led to slight changes in the reaction profile.

The free energy profiles for reaction in solvent calculated from eq 4 are shown in Figures 3 and 4. It can be seen that the difference in activation energy between the two principal reaction paths is large compared to the effect of optimizing in solvent.

Figure 5 shows part of the solvated profile for both model systems including the neutral substitution product, silyl peroxide

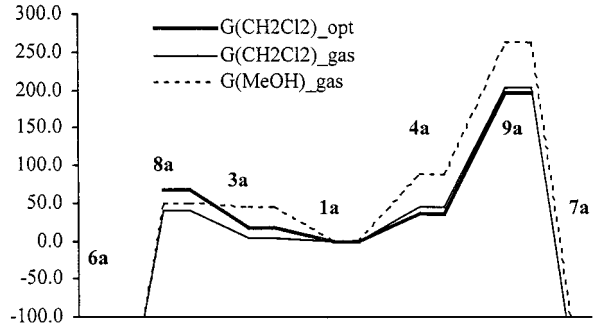

Figure 3. Solvated free energy profiles for oxidation of **1a**, kJ/mol.

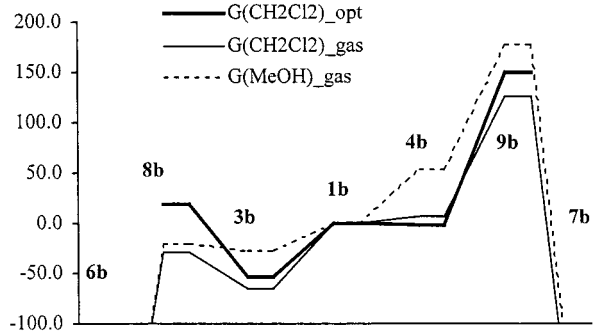

Figure 4. Solvated free energy profiles for oxidation of **1b**, kJ/mol.

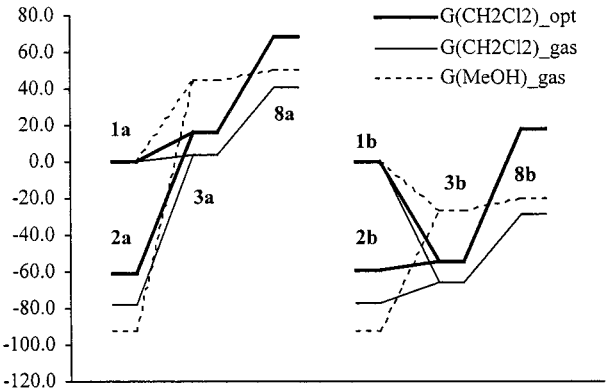

Figure 5. Solvated profiles from **2** to **8** for both model systems.

2. As opposed to the gas-phase results (Table 1), in solvent the formation of **2** from **1** is strongly favored. Under Curtin−Hammett conditions, the activation barrier is thus the energy difference between **8** and **2**, not **8** and **1**.

For the ground-state structures, the geometries obtained at the different levels of theory are very similar. The basic HF/6-31G* structures only display minor changes on optimization with a correlated method (B3LYP/6-31+G*) or in solvent (CPCM/UAHF at HF/6-31+G*), with bond lengths generally slightly longer at B3LYP. For transition states, the variations are larger, as expected from the larger range of TS energies obtained at different levels (Figures 1 and 2). Figure 6 depicts transition states **8** and **9** for both model systems, showing critical bond lengths from all three optimization levels.

The quality of the computed structures can also be assessed by comparison to identical or similar structures for which X-ray crystal structures have been determined (Table 3). A comparison of the optimized geometries of two key pentacoordinate compounds (**4a** and **4b**) to crystal structures for analogous fluorosilanes shows good agreement between theory and experiment, especially for the HF/6-31G*-derived geometries. We can be confident that the structures optimized at the HF/6-31G* level of theory are adequate for this study. The bond lengths calculated

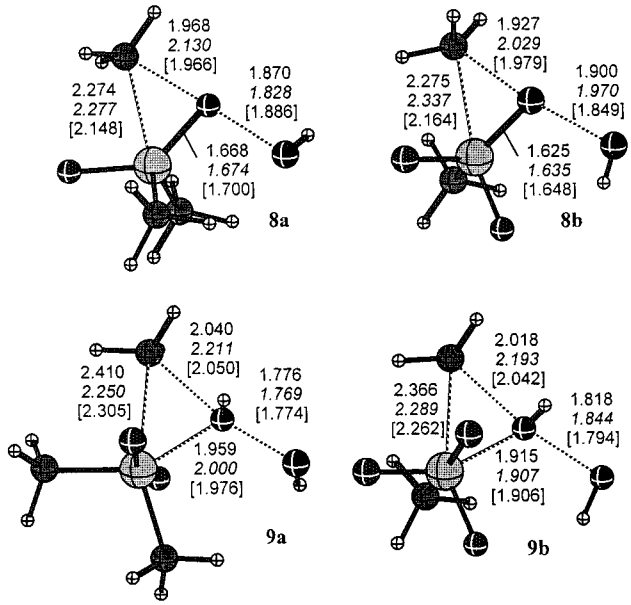

Figure 6. Transition state geometries at the HF/6-31G* level, with the lengths of the Si−O and the three reacting bonds shown. The values obtained from B3LYP and CPCM optimization are given in italics and bracketed, respectively.

Table 3. Comparison of Si−F Bond Lengths (Å)

compd	axial	equatorial	method
$[Me_3SiF_2]^-$	1.72−1.73		X-ray, ref 33
4a	1.73		HF/6-31G*
4a	1.80		B3LYP/6-31+G*
$[PhMeSiF_3]^-$	1.692	1.62	X-ray, ref 34
$[Ph_2SiF_3]^-$	1.696 (av)	1.655 (av)	X-ray, ref 35
4b	1.701	1.641	HF/6-31G*
4b	1.758	1.676	B3LYP/6-31+G*

at the B3LYP/6-31+G* level show a greater difference from experimental than do the HF-6-31G* geometries, ranging from 0.06 to 0.08 Å. However, the trends observed in the PES obtained at B3LYP are consistent with those we see in single-point calculations based on HF/6-31G* geometries.[30]

For the generation of hypervalent species **3**, **4**, and **5**, in which addition of OOH^- could occur through an axial or equatorial position, the lowest energy conformations of all possible isomers were analyzed at the semiempirical level. For the pentacoordinate species **3** and **4**, OOH^- added at the axial position, with pseudorotation of this substituent to an equatorial site upon methyl migration. The lowest energy conformations found for the hexacoordinate silane species are structurally similar: the geometries are octahedral (square bipyramidal), with the OOH cis to a fluoride. Attachment of HOO in a position diaxial to F tended to be slightly higher in energy, by up to 10 kJ/mol, for the hexacoordinate silanes **5a** and **5b**.

Discussion

Our goals were 2-fold: first, to consider plausible mechanisms for the rearrangement under both basic and neutral conditions that are consistent with Tamao's kinetic studies, and second, to examine the role of fluoride and increasing fluoride substitution in determining which path may be followed.

Consideration of Path A: A Simultaneous Addition/Rearrangement Transition State. A dimethylphenylsilane is

(30) Norrby, P.-O.; Rasmussen, T.; Haller, J.; Strassner, T.; Houk, K. N. *J. Am. Chem. Soc.* **1999**, *121*, 10186−10192.

replaced by an alcohol in a typical Fleming oxidation, and several sets of reagents and reaction conditions effect this transformation. In general, the phenyl substituent is removed by an electrophilic aromatic substitution, which serves to introduce an activating group (F or OAc, most commonly) on silicon. A tetravalent fluorosilane intermediate is isolated when HBF_4 is used in this first step, hence our choice of mono- and difluorosilanes (**1a** and **1b**, respectively) as models. The silane is then treated with an excess of both H_2O_2 and fluoride, or buffered peracid (AcOOH, NaOAc), or basic peracid (*m*-CPBA, Et_3N), and the alcohol is obtained after workup. Fleming suggests that the fluoride or acetate is displaced by peroxide anion (**1** → **2**), and the resulting tetravalent silane is reattacked by excess fluoride in solution, with concomitant migration of an alkyl group (Scheme 1, transition state A).[10] In our mechanistic scheme, **2** could result from direct displacement of fluoride from **1** by HOO^-, or via expulsion of fluoride from a pentavalent intermediate, **3**. Given the reported strength of the Si−F bond (bond dissociation energy: 810 kJ/mol), loss of fluoride by either mechanism seemed counter intuitive, but we attempted to determine if such losses could in fact occur. We then sought to locate transition state A, corresponding to simultaneous fluoride attack and rearrangement.

In the gas phase, formation of **2** from either **1** or **3** is endothermic (Table 2), which is not unexpected. The negatively charged fluoride has less surface area than HOO^- or **3** over which to distribute a negative charge, and thus fluoride generation is disfavored. In fact, of the three materials, **3** is the favored species in the gas phase. Approach of HOO^- to **1** always leads to formation of **3**, never to a direct S_N2-type displacement. Based solely on gas-phase energies, production of **2** might have been discounted. The solvent corrections are important, however, and in all cases formation of **2** becomes exothermic, demonstrating that consideration of the solvation of the ions is essential. Thus, the subsequent step, the simultaneous fluoride attack with methyl migration and hydroxide displacement (transition state A), needs to be considered. However, the calculations clearly show that addition of fluoride anion to **2** does not trigger a rearrangement, but simply reforms **3**. Keeping in mind that pentavalent silanes are at least transiently stable (depending on substituents), we moved to investigation of a mechanism that involves formation of a stable pentavalent silane *followed* by migration of the alkyl group with displacement of hydroxide (i.e. Path B).

Consideration of Path B: Attack and Rearrangement Under Basic Conditions. As pursuit of Path A indicated that **3** was a stable minimum, its methyl migration with hydroxide displacement was investigated (Figure 1: Path B, **1** → **3** → TS_B-(**8**) → **6**). We kept in mind Tamao's kinetic studies, in which pentavalent species are formed, the difluoride is more reactive than the monofluoride, and an excess of fluoride is required. In addition, the mechanism should be consistent with Fleming conditions (e.g. *m*-CPBA, Et_3N or AcOOH, NaOAc) which are basic but do not call for additional fluoride.

In the gas phase, the conversion of neutral **1** to pentavalent intermediate **3** is calculated to be exothermic by 158 kJ/mol for the monofluoride **3a** and 222 kJ/mol for the difluoride **3b**. Application of the solvent models damps the exothermicity of formation of **3** by a similar value (Table 1), making **1** and **3** more nearly isoenergetic (Figure 5). This difference between solvent and gas phase is not surprising. The HOO^- anion is not well stabilized in the gas phase, and combination with a neutral molecule yields an anion with the charge distributed over a larger surface area. Other workers have observed computationally the same phenomenon for the conversion of tetracoordinate to pentacoordinate silanes in the gas phase.[31]

For both substrates **3a** and **3b**, the effect of the solvent correction on the activation barrier to the transition states **8a** and **8b**, respectively, is noteworthy. In the gas phase, the free energy activation barrier to the rearrangement is 83 kJ/mol for **3a** and 109 kJ/mol for **3b**, but in solvent the local barriers are reduced to 37−73 kJ/mol in CH_2Cl_2 and to a neglible 5−7 kJ/mol in MeOH. The barrier is slightly higher for the difluoride **3b** than for monofluoride **3a**. However, the reactivity and activation barriers should also be considered in light of the possible preequilibria (Figure 5).

For both the mono- and difluoride, the ground state in solution is **2**. The barrier should be measured from this species, yielding activation free energies of 119 to 143 kJ/mol for the monofluoride (**2a** → **8a**) and 78 to 112 kJ/mol for the difluoride. Again, the total activation energy is in qualitative agreement with the observed rate difference between mono- and difluorides. It should also be remembered that all calculated free energies correspond to a standard state of 1 M. Decreasing the fluoride concentration will shift the equilibrium from **3** to **2**, increasing the activation barrier for the cases where **2** is the ground state, thus rationalizing the beneficial effect of added fluoride salt. We also note that under some conditions, product **6** will react with one more equivalent of fluoride to form **7**, depleting the fluoride concentration as the reaction progresses. This result is in perfect agreement with the observation that some reactions require stoichiometric fluoride salt addition.

Finally, the net conversion to **6** from **1** is highly exothermic, and the exothermicity is accentuated by the solvent model. Although the kinetics of the rearrangement under basic conditions have not been explicitly examined, Path B fits the experimental observations of Tamao in the order of fluoride reactivity, involvement of a pentavalent intermediate, and beneficial effect of additional fluoride. It is also consistent with Fleming procedures that employ basic peroxides and no additional fluoride for cases where the fluoride liberated from **3** is not absorbed by formation of **7**. Thus, a mechanism of peroxide attack and rapid fluoride equilibration (Curtin−Hammett conditions) followed by alkyl migration appears to be feasible.

Consideration of Path C: Attack and Rearrangement Under Neutral Conditions. Tamao's experimental examination of the oxidation mechanism under neutral conditions concludes that H_2O_2 approaches a pentavalent silicate, and migration of an alkyl substituent occurs with simultaneous water departure (Figure 1: Path C, **1** → **4** → TS_C-(**9**) → **7**). He postulates that fluoride plays a key role, not just in activating the silane toward nucleophilic attack by formation of the pentavalent intermediate, but also by serving as a hydrogen bond acceptor to assist in water formation. Thus, we sought to computationally confirm the mechanism under neutral conditions as well. Path C requires formation of a pentavalent species, **4**, as well as a transition state consistent with Tamao's mechanism, and observes the same order of reactivity of the initial fluorides **1a** and **1b**.

A transition state, TS_C-(**9**), was located which is consistent with that proposed by Tamao. The required features, pseudo-equatorial approach of H_2O_2, a hydrogen bond between H_2O_2 and a fluoride on silicon, and loss of H_2O, are all observed in this structure. The activation barriers in the gas phase are accessible, 77 kJ/mol for **4a** → **9a** and 61 kJ/mol for **4b** → **9b**. For this transition state, however, the solvent correction increases, rather than decreases, the barrier to rearrangement. In contrast to the TS_B-(**8**), this transition state does not gain

additional stability in solvent as the neutral leaving group (H_2O) is generated. TS_C-(**9**) differs from all other structures in the study by the presence of two intramolecular hydrogen bonds, providing a strong stabilization of the anionic charge in the gas phase, but a negligible contribution in solvent. The total effect is that TS_C-(**9**) is higher than TS_B-(**8**) by 100−200 kJ/mol in the solvents investigated. Thus, the current results strongly indicate that the reaction does not proceed via TS_C-(**9**). However, in the gas phase, and therefore presumably in very nonpolar solvents, TS_C-(**9**) is favored. Also, under conditions where the hydrogen peroxide is present only in neutral form (that is, acidic and/or nonpolar), path B would lack its essential reactant, and path C could presumably become operative.

Consideration of Path D: Rearrangement via a Hexacoordinated Silicate Dianion. We last investigated hydroperoxide anion (HOO^-) attack on the pentavalent fluorosilicates **4** to form stable, hexacoordinate silane dianions **5** (Scheme 1, path D). The hexacoordinate dianions **5** were located as stable minima, but the formation of a hexavalent intermediate **5** from both **4a** and **4b** is strongly endothermic in the gas phase. These findings are in accord with earlier gas-phase computational studies of hypervalent silicon anions, which also found the formation of the hexacoordinated sila-dianions to be quite endothermic.[31] Upon solvation correction, **5** is strongly stabilized, but is still disfavored. Formation of **5** requires hydroperoxide anion (HOO^-), and is thus competing with formation of **3** and subsequent rearrangement via **8**. It can be seen that in all cases, the postulated intermediate **5** is higher in energy than TS_B-(**8**) (Table 2), excluding paths via **5**.

Thus, the computational results suggest that species **4** is more likely to exist in equilibrium with **3** through anion exchange than to form a hexavalent intermediate **5**. In work unrelated to the silane oxidation mechanism, both stable pentavalent and hexavalent silicates have been isolated or characterized,[11] and these spectroscopic studies also indicate that substituents play a large role in the stability of penta- and hexavalent silicon. Gordon's computational work draws a similar conclusion: substituent effects are tremendously important in the stability of these hypervalent species.[31] The species that have been isolated are largely substituted with oxygen moieties, not alkyl groups. Substrates for the Tamao oxidation possess, at a minimum, two, if not three alkyl groups and only one or two alkoxy substituents at the outset.

Conclusions

Four proposed mechanisms for the peroxide oxidation of a silane to an alcohol were investigated both in the gas phase and with solvent corrections. The most likely mechanism is that in which attack by HOO^- forms a pentavalent silicate by addition to silicon, followed by migration of an alkyl group with simultaneous loss of hydroxide (**3** → TS_B-(**8**)). Formation and rearrangement of a hexavalent intermediate by Path D is less likely, as is a concerted displacement/rearrangement scheme (Path A). The mechanism proposed by Tamao (Path C) could possibly be operative under certain conditions, but in general it is strongly disfavored compared to path B. The solvent corrections are significant for these reactions involving ions, and tend to damp the highly exothermic combination of ions to form the initial pentavalent species. It is noticeable that a study without either solvation treatment or diffuse functions in the basis would have found the Tamao mechanism as the most likely. However, the strong hydrogen bonds that favor this path in the gas phase have much less influence when competition with solvent intrudes.

The same computational techniques could be applied to two related issues of organosilane oxidation chemistry. The role of alkoxysilanes in the oxidation, either as starting materials or as reactive intermediates, requires further investigation. In addition, computational and experimental studies are being conducted to determine nitrogen compounds could behave in a fashion analogous to peroxide in effecting a silane-to-amine conversion.[32]

Acknowledgment. M.M.M. thanks Research Corporation (CC3865) and Grinnell College for support of this work. P.O.N. is grateful to the Danish Technical Research Council for a generous grant. M.M.M. thanks Prof. Olaf Wiest, Marisa Kozlowski, and Mark Gordon for helpful discussions.

Supporting Information Available: Cartesian coordinates of HF/6-31G* optimized geometries and calculated total energies (HF/6-31G*//HF/6-31G*, MP2/6-31G**//HF/6-31G*, HF/6-31G**//HF/6-31G*, HF/6-31+G*//HF/6-31G*, MP2/6-311+G**//HF/6-31G*, and B3LYP/6-31+G*//B3LYP/6-31+G*) for all structures (PDF). This material is available free of charge via the Internet at http://pubs.acs.org.

JA001400P

(31) Gordon, M. S.; Davis, L. P.; Burggraf, L. W. In *Advances in Gas-Phase Ion Chemistry*; JAI Press: Greenwich, CT, 1992; Vol. 1, pp 203−223.

(32) For an example of computer-aided reaction design, see: Fukuda, S.; Akiyoshi, Y.; Hori, K. *J. Org. Chem.* **1999**, *64*, 4768−4774.

(33) Scherbaum, F.; Huber, B.; Muller, G.; Schmidbaur, H. *Angew. Chem., Int. Ed. Engl.* **1988**, *27*, 1542.

(34) Harland, J. J.; Payne, J. S.; Day, R. O.; Holmes, R. R. *Inorg. Chem.* **1987**, *26*, 760.

(35) Schomburg, D.; Krebs, R. *Inorg. Chem.* **1984**, *23*, 1378.